Eur. Phys. J. C 48, 685–698 (2006)
DOI 10.1140/epjc/s10052-006-0017-5

THE EUROPEAN PHYSICAL JOURNAL C

Regular Article – Experimental Physics

Test of colour reconnection models using three-jet events in hadronic Z decays

The ALEPH Collaboration

S. Schael[1], R. Barate[2], R. Brunelière[2], I. De Bonis[2], D. Decamp[2], C. Goy[2], S. Jézéquel[2], J.-P. Lees[2], F. Martin[2], E. Merle[2], M.-N. Minard[2], B. Pietrzyk[2], B. Trocmé[2], S. Bravo[3], M.P. Casado[3], M. Chmeissani[3], J.M. Crespo[3], E. Fernandez[3], M. Fernandez-Bosman[3], L. Garrido[3,a], M. Martinez[3], A. Pacheco[3], H. Ruiz[3], A. Colaleo[4], D. Creanza[4], N. De Filippis[4], M. de Palma[4], G. Iaselli[4], G. Maggi[4], M. Maggi[4], S. Nuzzo[4], A. Ranieri[4], G. Raso[4,b], F. Ruggieri[4], G. Selvaggi[4], L. Silvestris[4], P. Tempesta[4], A. Tricomi[4,c], G. Zito[4], X. Huang[5], J. Lin[5], Q. Ouyang[5], T. Wang[5], Y. Xie[5], R. Xu[5], S. Xue[5], J. Zhang[5], L. Zhang[5], W. Zhao[5], D. Abbaneo[6], T. Barklow[6,d], O. Buchmüller[6,d], M. Cattaneo[6], B. Clerbaux[6,e], H. Drevermann[6], R.W. Forty[6], M. Frank[6], F. Gianotti[6], J.B. Hansen[6], J. Harvey[6], D.E. Hutchcroft[6,f], P. Janot[6], B. Jost[6], M. Kado[6,g], P. Mato[6], A. Moutoussi[6], F. Ranjard[6], L. Rolandi[6], D. Schlatter[6], F. Teubert[6], A. Valassi[6], I. Videau[6], F. Badaud[7], S. Dessagne[7], A. Falvard[7,h], D. Fayolle[7], P. Gay[7], J. Jousset[7], B. Michel[7], S. Monteil[7], D. Pallin[7], J.M. Pascolo[7], P. Perret[7], J.D. Hansen[8], J.R. Hansen[8], P.H. Hansen[8], A.C. Kraan[8], B.S. Nilsson[8], A. Kyriakis[9], C. Markou[9], E. Simopoulou[9], A. Vayaki[9], K. Zachariadou[9], A. Blondel[10,i], J.-C. Brient[10], F. Machefert[10], A. Rougé[10], H. Videau[10], V. Ciulli[11], E. Focardi[11], G. Parrini[11], A. Antonelli[12], M. Antonelli[12], G. Bencivenni[12], F. Bossi[12], G. Capon[12], F. Cerutti[12], V. Chiarella[12], P. Laurelli[12], G. Mannocchi[12,j], G.P. Murtas[12], L. Passalacqua[12], J. Kennedy[13], J.G. Lynch[13], P. Negus[13], V. O'Shea[13], A.S. Thompson[13], S. Wasserbaech[14], R. Cavanaugh[15,k], S. Dhamotharan[15,l], C. Geweniger[15], P. Hanke[15], V. Hepp[15], E.E. Kluge[15], A. Putzer[15], H. Stenzel[15], K. Tittel[15], M. Wunsch[15,m], R. Beuselinck[16], W. Cameron[16], G. Davies[16], P.J. Dornan[16], M. Girone[16,n], N. Marinelli[16], J. Nowell[16], S.A. Rutherford[16], J.K. Sedgbeer[16], J.C. Thompson[16,o], R. White[16], V.M. Ghete[17], P. Girtler[17], P. Jussel[17], E. Kneringer[17], D. Kuhn[17], G. Rudolph[17], E. Bouhova-Thacker[18], C.K. Bowdery[18], D.P. Clarke[18], G. Ellis[18], A.J. Finch[18], F. Foster[18], G. Hughes[18], R.W.L. Jones[18], M.R. Pearson[18], N.A. Robertson[18], M. Smizanska[18], O. van der Aa[19], C. Delaere[19,p], G.Leibenguth[19,q], V. Lemaitre[19,r], U. Blumenschein[20], F. Hölldorfer[20], K. Jakobs[20], F. Kayser[20], A.-S. Müller[20], B. Renk[20], H.-G. Sander[20], S. Schmeling[20], H. Wachsmuth[20], C. Zeitnitz[20], T. Ziegler[20], A. Bonissent[21], P. Coyle[21], C. Curtil[21], A. Ealet[21], D. Fouchez[21], P. Payre[21], A. Tilquin[21], F. Ragusa[22], A. David[23], H. Dietl[23,s], G. Ganis[23,t], K. Hüttmann[23], G. Lütjens[23], W. Männer[23,s], H.-G. Moser[23], R. Settles[23], M. Villegas[23], G. Wolf[23], J. Boucrot[24], O. Callot[24], M. Davier[24], L. Duflot[24], J.-F. Grivaz[24], P. Heusse[24], A. Jacholkowska[24,u], L. Serin[24], J.-J. Veillet[24], P. Azzurri[25], G. Bagliesi[25], T. Boccali[25], L. Foà[25], A. Giammanco[25], A. Giassi[25], F. Ligabue[25], A. Messineo[25], F. Palla[25], G. Sanguinetti[25], A. Sciabà[25], G. Sguazzoni[25], P. Spagnolo[25], R. Tenchini[25], A. Venturi[25], P.G. Verdini[25], O. Awunor[26], G.A. Blair[26], G. Cowan[26], A. Garcia-Bellido[26], M.G. Green[26], T. Medcalf[26,v], A. Misiejuk[26], J.A. Strong[26], P. Teixeira-Dias[26], R.W. Clifft[27], T.R. Edgecock[27], P.R. Norton[27], I.R. Tomalin[27], J.J. Ward[27], B. Bloch-Devaux[28], D. Boumediene[28], P. Colas[28], B. Fabbro[28], E. Lançon[28], M.-C. Lemaire[28], E. Locci[28], P. Perez[28], J. Rander[28], B. Tuchming[28], B. Vallage[28], A.M. Litke[29], G. Taylor[29], C.N. Booth[30], S. Cartwright[30], F. Combley[30,v], P.N. Hodgson[30], M. Lehto[30], L.F. Thompson[30], A. Böhrer[31], S. Brandt[31], C. Grupen[31], J. Hess[31], A. Ngac[31], G. Prange[31], C. Borean[32], G. Giannini[32], H. He[33], J. Putz[33], J. Rothberg[33], S.R. Armstrong[34], K. Berkelman[34], K. Cranmer[34], D.P.S. Ferguson[34], Y. Gao[34,w], S. González[34], O.J. Hayes[34], H. Hu[34], S. Jin[34], J. Kile[34], P.A. McNamara III[34], J. Nielsen[34], Y.B. Pan[34], J.H. von Wimmersperg-Toeller[34], W. Wiedenmann[34], J. Wu[34], S.L. Wu[34], X. Wu[34], G. Zobernig[34], G. Dissertori[35]

[1] Physikalisches Institut, RWTH-Aachen, 52056 Aachen, Germany
[2] Laboratoire de Physique des Particules (LAPP), IN^{2}P^3-CNRS, 74019 Annecy-le-Vieux Cedex, France
[3] Institut de Física d'Altes Energies, Universitat Autònoma de Barcelona, 08193 Bellaterra (Barcelona), Spain[x]
[4] Dipartimento di Fisica, INFN Sezione di Bari, 70126 Bari, Italy
[5] Institute of High Energy Physics, Academia Sinica, Beijing, P.R. China[y]
[6] European Laboratory for Particle Physics (CERN), 1211 Geneva 23, Switzerland
[7] Laboratoire de Physique Corpusculaire, Université Blaise Pascal, IN^{2}P^3-CNRS, Clermont-Ferrand, 63177 Aubière, France
[8] Niels Bohr Institute, 2100 Copenhagen, Denmark[z]
[9] Nuclear Research Center Demokritos (NRCD), 15310 Attiki, Greece
[10] Laoratoire Leprince-Ringuet, Ecole Polytechnique, IN^{2}P^3-CNRS, 91128 Palaiseau Cedex, France
[11] Dipartimento di Fisica, Università di Firenze, INFN Sezione di Firenze, 50125 Firenze, Italy
[12] Laboratori Nazionali dell'INFN (LNF-INFN), 00044 Frascati, Italy

[13] Department of Physics and Astronomy, University of Glasgow, Glasgow G12 8QQ, UK[aa]
[14] Utah Valley State College, Orem, 84058, USA
[15] Kirchhoff-Institut für Physik, Universität Heidelberg, 69120 Heidelberg, Germany[ab]
[16] Department of Physics, Imperial College, London SW7 2BZ, UK[aa]
[17] Institut für Experimentalphysik, Universität Innsbruck, 6020 Innsbruck, Austria[ac]
[18] Department of Physics, University of Lancaster, Lancaster LA1 4YB, UK[aa]
[19] Institut de Physique Nucléaire, Département de Physique, Université Catholique de Louvain, 1348 Louvain-la-Neuve, Belgium
[20] Institut für Physik, Universität Mainz, 55099 Mainz, Germany[ab]
[21] Centre de Physique des Particules de Marseille, Univ. Méditerranée, IN^{2}P^3-CNRS, 13288 Marseille, France
[22] Dipartimento di Fisica, Università di Milano e INFN Sezione di Milano, 20133 Milano, Italy
[23] Max-Planck-Institut für Physik, Werner-Heisenberg-Institut, 80805 München, Germany[ab]
[24] Laboratoire de l'Accélérateur Linéaire, Université de Paris-Sud, IN^{2}P^3-CNRS, 91898 Orsay Cedex, France
[25] Dipartimento di Fisica dell'Università, INFN Sezione di Pisa, e Scuola Normale Superiore, 56010 Pisa, Italy
[26] Department of Physics, Royal Holloway & Bedford New College, University of London, Egham, Surrey TW20 OEX, UK[aa]
[27] Particle Physics Dept., Rutherford Appleton Laboratory, Chilton, Didcot, Oxon OX11 OQX, UK[aa]
[28] CEA, DAPNIA/Service de Physique des Particules, CE-Saclay, 91191 Gif-sur-Yvette Cedex, France[ad]
[29] Institute for Particle Physics, University of California at Santa Cruz, Santa Cruz, CA 95064, USA[ae]
[30] Department of Physics, University of Sheffield, Sheffield S3 7RH, UK[aa]
[31] Fachbereich Physik, Universität Siegen, 57068 Siegen, Germany[ab]
[32] Dipartimento di Fisica, Università di Trieste e INFN Sezione di Trieste, 34127 Trieste, Italy
[33] Experimental Elementary Particle Physics, University of Washington, Seattle, WA 98195, USA
[34] Department of Physics, University of Wisconsin, Madison, WI 53706, USA[af]
[35] Institute for Particle Physics, ETH Hönggerberg, 8093 Zürich, Switzerland

Received: 25 April 2006 / Revised version: 20 June 2006 /
Published online: 24 October 2006 –

Abstract. Hadronic Z decays into three jets are used to test QCD models of colour reconnection (CR). A sensitive quantity is the rate of gluon jets with a gap in the particle rapidity distribution and zero jet charge. Gluon jets are identified by either energy-ordering or by tagging two b-jets. The rates predicted by two string-based tunable CR models, one implemented in JETSET (the GAL model), the other in ARIADNE, are too high and disfavoured by the data, whereas the rates from the corresponding non-CR standard versions of these generators are too low. The data can be described by the GAL model assuming a small value for the R_0 parameter in the range $0.01 - 0.02$.

[a] Permanent address: Universitat de Barcelona, 08208 Barcelona, Spain
[b] Now at Dipartimento di Fisica e Tecnologie Relative, Università di Palermo, Palermo, Italy
[c] Also at Dipartimento di Fisica di Catania and INFN Sezione di Catania, 95129 Catania, Italy
[d] Now at SLAC, Stanford, CA 94309, USA
[e] Now at Institut Inter-universitaire des hautes Energies (IIHE), CP 230, Université Libre de Bruxelles, 1050 Bruxelles, Belgique
[f] Now at Liverpool University, Liverpool L69 7ZE, UK
[g] Now at Fermilab, PO Box 500, MS 352, Batavia, IL 60510, USA
[h] Now at Groupe d' Astroparticules de Montpellier, Université de Montpellier II, 34095 Montpellier, France
[i] Now at Departement de Physique Corpusculaire, Université de Genève, 1211 Genève 4, Switzerland
[j] Also IFSI sezione di Torino, INAF, Italy
[k] Now at University of Florida, Department of Physics, Gainesville, Florida 32611-8440, USA
[l] Now at BNP Paribas, 60325 Frankfurt am Mainz, Germany
[m] Now at SAP AG, 69185 Walldorf, Germany
[n] Also at CERN, 1211 Geneva 23, Switzerland
[o] Supported by the Leverhulme Trust
[p] Research Fellow of the Belgium FNRS
[q] Supported by the Federal Office for Scientific, Technical and Cultural Affairs through the Interuniversity Attraction Pole P5/27
[r] Research Associate of the Belgium FNRS
[s] Now at Henryk Niewodniczanski Institute of Nuclear Physics, Polish Academy of Sciences, Cracow, Poland
[t] Now at CERN, 1211 Geneva 23, Switzerland
[u] Also at Groupe d'Astroparticules de Montpellier, Université de Montpellier II, 34095, Montpellier, France
[v] Deceased
[w] Also at Department of Physics, Tsinghua University, Beijing, P.R. China
[x] Supported by CICYT, Spain
[y] Supported by the National Science Foundation of China
[z] Supported by the Danish Natural Science Research Council
[aa] Supported by the UK Particle Physics and Astronomy Research Council
[ab] Supported by Bundesministerium für Bildung und Forschung, Germany

1 Introduction

A description of the hadronisation of a multiparton system requires specification of the colour connections among the partons. These can be modified by higher-order interference or non-perturbative effects in QCD, a phenomenon commonly called colour reconnection (CR) [1]. These effects can only be studied within the framework of specific models. The present interest in CR arises from the precise measurement of the W boson mass in $W^+W^- \to q\bar{q}q\bar{q}$ events in e^+e^- collisions at LEP2 energies. In this fully hadronic final state possible CR effects among the decay products of the two W bosons contribute the largest systematic uncertainty to m_{W} [2]. Direct information on CR in this channel is obtained from inter-jet particle flow studies [3, 4] and/or from the W mass itself by comparing different jet algorithms [5, 6]. Due to limited statistics only extreme models can be excluded.

CR effects might also appear within a colour singlet system like the one produced in the reaction $e^+e^- \to q\bar{q}$(+gluons) on the Z resonance at LEP1 where high statistics data are available. To search for CR effects one has to look for hadronic variables which are sensitive to the colour flow in an event. Following a proposal in [7], the OPAL collaboration has shown that gluon jets with a rapidity gap and zero jet charge, identified in events of the type $Z \to 3$ jets, provide a sensitive means to search for CR effects, and concluded that two string-based CR models are disfavoured by their data [8, 9]. The L3 collaboration, employing angular gaps in the inter-jet regions of symmetric three-jet events, arrived at a similar conclusion [10]. By comparing quark with gluon jets, the DELPHI collaboration found that also the standard colour string model (without CR) cannot adequately describe the fraction of neutral gluon jets with a rapidity gap [11]. They suggest a contribution either from a colour octet neutralisation mechanism [12] or, alternatively, from colour reconnection.

In the present paper the variables proposed in [8] are used both to test CR models and to investigate the discrepancy reported in [11]. The data were collected by the ALEPH detector at LEP1. The data are compared to QCD Monte Carlo model calculations with and without implementation of CR and with parameters tuned to global properties of hadronic Z decays. Gluon jets from three-jet events are identified by either energy-ordering or by anti-b tagging. The rate of neutral jets is studied as a function of the rapidity gap size. Quark jets from the same events are used for purposes of comparison. The influence of Bose–Einstein correlations is also investigated.

[ac] Supported by the Austrian Ministry for Science and Transport

[ad] Supported by the Direction des Sciences de la Matière, C.E.A.

[ae] Supported by the US Department of Energy, grant DE-FG03-92ER40689

[af] Supported by the US Department of Energy, grant DE-FG0295-ER40896

2 QCD models for colour reconnection

Some basic properties of the non-perturbative CR models to be discussed in this paper are listed in Table 1. The first detailed theoretical study of CR was carried out by Sjöstrand and Khoze (SK) [13, 14] in the context of a possible cross-talk among the hadronically decaying W bosons in W pair production and its effect on the W mass measurement. The perturbative QCD contribution from one-gluon exchange was found to be negligible, but there could be a sizeable non-perturbative contribution. Using the leading-log approximation (LLA), each $q\bar{q}$ system is evolved into a parton shower which, in the large-N_{C} limit (where N_{C} is the number of colours), determines a sequence of colour-connected partons (quarks and gluons) which is used to draw the colour string. The authors developed a non-perturbative reconnection model, implemented [15] in the PYTHIA generator version 6, based on the space-time overlap of the colour strings. The model variants SKI and SKII may be considered as two extreme descriptions of the colour string topology. In SKI, strings are assumed to be extended flux tubes. The probability to reconnect two strings is related to the overlap integral I and is given by

$$P_{\mathrm{reco}} = 1 - \exp\left(-k_{\mathrm{I}} \cdot I\right)$$

where k_{I} is a free parameter. In the SKII model the information is contained in thin vortex lines. Reconnection is assumed to take place with unit probability if they cross each other. The fact that the fraction of reconnected events is predicted in model SKII can be used to fix the parameter k_{I} such that this fraction is the same in the two models ($k_{\mathrm{I}} = 0.65$). In the SKI model, CR effects would in principle also be possible within colour singlet (CS) systems like W or Z decays, but they have not been implemented and are thus not testable. It is remarkable that the SKII model predicts that such reconnections should not occur at all within singlet systems since the partons emerge from a single vertex [16].

The ARIADNE generator, version 4 [17], which is based on the colour dipole model, provides options for colour reconnection [18]. Considering all pairs of non-adjacent dipoles, reconnections take place with probability $1/N_{\mathrm{C}}^2$ if the total string length λ decreases. The λ measure is defined from the four-momenta of n colour-ordered partons:

$$\lambda = \sum_{i=1}^{n-1} \log\left(\left(p_i + p_{i+1}\right)^2 / m_0^2\right)$$

with $m_0 = 1\,\mathrm{GeV}$. In the program, N_{C}^2 may be considered a free parameter, normally set to 9. The option AR1 used in this paper enables reconnections only within colour singlet systems, whereas AR2 is foreseen for reconnections also between CS systems like W pairs.

The model due to Rathsman [19] is based on the so-called generalized area law (GAL). The total area of

Table 1. Properties of colour reconnection models

model	criterion of reconnection	free parameter	value	effect in $Z \to q\bar{q}$
SKI	space-time overlap of flux tubes	k_{I}	0.65	not implemented
SKII	crossing of vortex lines	–	–	No
ARIADNE AR1	reduce total string length λ	P_{reco}	1/9	Yes
GAL (Rathsman)	reduce total string area A	R_0	0.1	Yes
HERWIG	reduce cluster size in space-time	P_{reco}	1/9	Yes

a string is the sum of the areas of its pieces:

$$A = \sum_{i=1}^{n-1} \left((p_i + p_{i+1})^2 - (m_i + m_{i+1})^2 \right) .$$

At the end of the parton shower, pairs of string pieces are allowed to reconnect with probability

$$P_{\mathrm{reco}} = R_0 \left(1 - \exp\left(-b \Delta A\right)\right) ,$$
$$\text{where} \quad \Delta A = \max\left(0, A - A_{\mathrm{reco}}\right) . \qquad (1)$$

A_{reco} is the area after a colour rearrangement and the positive parameter b is one of the two parameters of the Lund symmetric fragmentation function. The phenomenological parameter R_0 should be of order $1/N_{\mathrm{C}}^2$. Its value has been determined by the author to be 0.10 from a comparison of the model to HERA data on the diffractive structure function of the proton. The Rathsman program is interfaced with PYTHIA(JETSET) version 5.7 [20].

The HERWIG generator, version 6.1 [21] or higher, offers a quite different concept for colour reconnection based on the space-time structure of an event at the partonic level. The relevant quantity is the cluster size defined as the Lorentz invariant space-time distance between the calculated production points of the quark and the antiquark forming a cluster. A reconnection among pairs of non-adjacent clusters is performed with probability $P_{\mathrm{reco}} = 1/9$ if the sum of the squared cluster sizes is lowered. On average, colour reconnection in this model leads to higher cluster masses.

3 QCD model tuning

Multi-hadronic final states are described by QCD Monte Carlo generators which contain a number of free parameters. These have to be determined from fits to data. This has been done extensively using event-shape, charged particle momentum and identified hadron momentum distributions measured by ALEPH in inclusive Z decays in order to check the overall description of the data and to obtain optimal values for the free parameters [22]. This section describes the tuning of the QCD generators when including colour reconnection. One of the effects of CR is that the average particle multiplicity changes slightly. For example, the average charged particle multiplicity, $\langle n_{\mathrm{ch}} \rangle$, changes by -2%, -1% and $+1\%$ for the GAL, AR1 and HW-CR models, respectively, as compared to the non-reconnected versions without changing any fragmentation parameters. Therefore the most important fragmentation parameters have been re-tuned for the colour reconnected versions of JETSET(GAL), ARIADNE and HERWIG. The tuning of HERWIG is described in more detail in [23]. The best fit values of the parameters are given in Tables 2–4 and the χ^2 values are summarized in Table 5. The results from the standard, non-reconnected versions are also included in the tables. For JETSET and ARIADNE, the string fragmentation parameters controlling the spin, flavour and type of the produced hadrons and the heavy quark fragmentation parameters ϵ_c, ϵ_b are taken from Table 8 of [22]. The tuning of JETSET including a simulation of Bose–Einstein correlations (model BE_{32}) is described in [24]. Also given in Tables 2–4 are the predicted charged particle multiplicities in hadronic events to be compared to the measured value 20.91 ± 0.22 [22].

Table 2. Tuned ARIADNE 4.08 parameters without (AR0) and with inclusion of CR (AR1). Any parameter given without error is fixed during the fit procedure. The fraction of reconnected events is given in the last line

parameter	MC name	AR0	AR1
CR option	MSTA(35)	0	1
N_C^2	PARA(26)	–	9
Λ (GeV)	PARA(1)	0.229 ± 0.003	0.230 ± 0.003
$p_{\mathrm{T,min}}$ (GeV)	PARA(3)	0.79 ± 0.05	0.79 ± 0.02
σ (GeV)	PARJ(21)	0.358 ± 0.009	0.353 ± 0.009
a	PARJ(41)	0.40	0.40
b $(\mathrm{GeV})^{-2}$	PARJ(42)	0.825 ± 0.024	0.758 ± 0.015
$\langle n_{\mathrm{ch}} \rangle$		20.58	20.61
f(reco)		–	0.15

Table 3. Tuned JETSET 7.4 parameters without and with inclusion of CR using the GAL model. Azimuthal isotropy in the parton shower is assumed (MSTJ(46)=0), since this option gives a better fit to the data. Any parameter given without error is fixed during the fit procedure. The fraction of reconnected events is given in the last line

parameter	MC name	JETSET	+GAL	+GAL
R_0	PARP(188)	–	0.039 ± 0.011	0.10
Λ (GeV)	PARJ(81)	0.312 ± 0.004	0.307 ± 0.006	0.306 ± 0.006
Q_0 (GeV)	PARJ(82)	1.50 ± 0.07	1.57 ± 0.08	1.79 ± 0.04
σ (GeV)	PARJ(21)	0.365 ± 0.009	0.364 ± 0.009	0.362 ± 0.009
a	PARJ(41)	0.40	0.40	0.40
b $(\mathrm{GeV})^{-2}$	PARJ(42)	0.900 ± 0.018	0.815 ± 0.026	0.724 ± 0.014
$\langle n_{\mathrm{ch}} \rangle$		20.64	20.65	20.67
f(reco)		–	0.10	0.18

Table 4. Tuned HERWIG 6.1 parameters without and with inclusion of CR. Two cluster model parameters, CLSMR and PSPLT, have been made flavour-dependent in order to better describe the measured B-meson fragmentation function. The D-wave meson multiplets are switched off. Any parameter given without error is fixed during the fit procedure. The fraction of reconnected events is given in the last line

parameter	MC name	HW0	HW-CR
P_{reco}	PRECO	0	1/9
min. virtuality (GeV^2)	VMIN2	–	0.1
Λ (GeV)	QCDLAM	0.190 ± 0.005	0.187 ± 0.005
gluon mass (GeV)	RMASS(13)	0.77 ± 0.01	0.79 ± 0.01
max. cluster mass (GeV)	CLMAX	3.39 ± 0.08	3.40 ± 0.08
angular smearing, dusc	CLSMR(1)	0.59 ± 0.03	0.66 ± 0.04
angular smearing, b	CLSMR(2)	0	0
power in cluster splitting, dusc	PSPLT(1)	0.945 ± 0.018	0.886 ± 0.017
power in cluster splitting, b	PSPLT(2)	0.33	0.32
decuplet baryon weight	DECWT	0.71 ± 0.06	0.70 ± 0.06
$\langle n_{\mathrm{ch}} \rangle$		20.96	20.98
f(reco)		–	0.08

Table 5. χ^2 values for the event-shape and charged particle momentum distributions used in the global fits. The total χ^2 values for the fits using restricted regions are given in the last line

	model	JETSET	GAL	GAL	AR0	AR1	HW0	HW-CR
	CR par.	0	0.04	0.10	0	1/9	0	1/9
distribution	bins							
sphericity, S	23	5	7	17	27	24	107	127
aplanarity, A	16	91	117	132	44	60	76	93
thrust, T	21	51	21	8	15	12	378	411
minor, T_{minor}	18	76	99	130	64	81	162	200
Feynman x_p	46	196	171	183	239	211	370	365
$p_{\mathrm{t,out}}$	19	1067	1010	1023	864	730	110	116
$p_{\mathrm{t,in}}$	25	107	63	70	156	73	171	164
sum	168	1592	1488	1563	1409	1190	1374	1476
with cuts	137	355	304	382	372	299	–	–

The multidimensional fitting method is described in [22]. The set of distributions used in the fits is listed in Table 5. The experimental distributions of these variables, corrected for detector and ISR effects, are those presented in [22] based on data collected in 1992. They are combined with data from the Z peak running in 1993 in order to increase the statistics to about 1 million hadronic events. The systematic errors are those evaluated for the 1992 sample. Since the total errors are dominated by systematics and since the systematic uncertainties are only rough estimates, the χ^2 values given in Table 5 should only be considered as a relative measure of the fit quality. In performing the fits of JETSET(+GAL) and ARIADNE, certain regions are excluded where these models clearly deviate from the data (the tails of the out-of-plane quantities $A \geq 0.06, T_{\mathrm{minor}} \geq 0.20, p_{\mathrm{t,out}} \geq 0.7\,\mathrm{GeV}$ and the very low $x_p \leq 0.014$). For the HERWIG fits the momentum spectra of non-strange and strange mesons as well as baryons are included in the set of distributions.

The large overall χ^2 values indicate that, despite parameter tuning, it is very difficult for the models to reproduce the data with a 1 to 2% accuracy. The JETSET and ARIADNE models underestimate the $p_{\mathrm{t,out}}$ tail by up to 30% with deviations typically around 10σ. This distribution is much better described by the HERWIG model. On the other hand, the distributions of sphericity and thrust, and of the scaled momenta, x_p, of charged particles are better described by JETSET or ARIADNE. HERWIG shows a significant excess (10σ) of low-thrust events and does not adequately describe the production of heavier particles like K-mesons and baryons.

The total uncertainties of the parameters in Tables 2–4 are determined as follows. First, the systematic uncertainties of the fitted distributions are included in the χ^2 minimization and thus propagated into an uncertainty on the parameters. Second, the fit procedure is changed by varying the fit regions and, in the case of HERWIG, the set of baryons included in the fit. The largest changes in the fitted parameters are added quadratically to the first contributions.

In order to test whether or not colour reconnection improves the overall description, the CR parameter of each model is fitted simultaneously with the other fragmentation parameters. The fit of the JETSET+GAL model has a χ^2 minimum with respect to the CR parameter R_0 at approximately 0.04. If this parameter is fixed at the recommended value of 0.10, the changes in the other parameters are mainly a larger value for the parton shower cut-off Q_0 and a smaller value for the b parameter. The optimal value for the CR parameter N_{C}^2 in the AR1 model is 8.4 ± 1.1, consistent with the default value of 9. Although the changes in total χ^2 are not large, the distributions of global variables show a slight preference for the string-based colour reconnection models. For the HERWIG-CR model, the χ^2 increases continuously with increasing P_{reco} parameter. However, the global variables like event-shape and particle momentum distributions considered here may not be specific enough for testing CR models.

4 Effects of colour reconnection in $Z \rightarrow$ hadrons

According to the string-based models AR1 and GAL, colour reconnection leads to shorter strings and thus to less particle multiplicity, on average. The changes of particle multiplicity and of the particle momentum distributions can be compensated, at least partially, by re-tuning the important fragmentation parameters. Clearly, more specific variables are needed to test CR models.

Studies of AR1 and GAL at the generator level show that the fraction of events with one or more reconnections, f(reco), strongly rises with the number of partons and with the number of hadronic jets in the event. Also, a minimum of four partons in the final state are needed to perform a reconnection. This suggests that CR is related to the presence of gluon jets. The simplest configuration which is expected to be favourable for testing CR models is therefore a three-jet event with one of the jets being a well separated and energetic gluon jet.

It is therefore important to check how well the gluon jet is described by the QCD models. The properties of gluon jets in comparison to those of quark jets have been studied in great detail at LEP [9, 25–29]. These studies include the fragmentation function and its scale dependence, the distributions of particle multiplicity and rapidity and the sub-jet structure. In general, good agreement between the data and the QCD model predictions is found. An exception is the fragmentation function at large x where the predictions are systematically low [25, 29].

A very specific and rare class of three-jet events in which the gluon jet exhibits a rapidity gap and in which the hadronic system beyond the gap has zero electric charge, has been proposed by the OPAL collaboration [8], referring to theoretical ideas of [7], as a signature for possible effects of colour octet neutralisation or colour reconnection. If a reconnection occurs according to the GAL or AR1 models, a gluon jet, which in general consists of several gluons, often hadronizes as a closed string separated from the $q\bar{q}$ string by a rapidity gap. The signature is an increased rate of gluon jets exhibiting a rapidity gap and zero electric charge of the system beyond the gap.

5 ALEPH detector, data and Monte Carlo samples

A description of the detector and its performance can be found elsewhere [30, 31]. Charged particles are detected in the central part consisting of a precision silicon strip detector (VDET), a cylindrical drift chamber (ITC) and a large time projection chamber (TPC). Jets originating from heavy quarks, in particular b-quarks, are identified with a lifetime tagging algorithm which takes advantage of the 3-dimensional impact parameter resolution of charged particle tracks. The tracking chambers are surrounded by the electromagnetic calorimeter (ECAL) located inside the magnet coil, and the hadronic calorimeter (HCAL).

Table 6. Statistics generated for each QCD Monte Carlo model

QCD model	million events
JETSET	7.6
JETSET+GAL, $R_0 = 0.04$	0.5
JETSET+GAL, $R_0 = 0.10$	3.4
JETSET+BE$_{32}$	0.5
ARIADNE AR0	3.4
ARIADNE AR1	3.4
HERWIG	0.5
HERWIG CR	0.5

The information from the tracking detectors and the calorimeters is combined in an energy-flow algorithm [31]. This algorithm provides, for each event, a list of reconstructed objects, classified as charged particles, photons and neutral hadrons, and called *energy flow objects* in the following. The pion mass is assigned to charged particles and zero mass to neutral particles. Objects reconstructed in the luminosity detectors are omitted.

Multihadronic Z decays are preselected by requiring at least five good charged tracks whose energy sum exceeds 10% of the center-of-mass energy, $E_{\rm cm}$. Good tracks are defined as originating close to the interaction point (with transverse impact parameter $|d_0| < 2$ cm and longitudinal impact parameter $|z_0| < 10$ cm), having at least four TPC hits and a polar angle such that $|\cos\theta| < 0.95$. Residual backgrounds from τ pair and $\gamma\gamma$ events are reduced to a negligible level by requiring the events to have at least 14 energy flow objects whose energy sum, $E_{\rm vis}$, exceeds 50% of $E_{\rm cm}$. This selection yields 3 378 000 hadronic events from the ALEPH data collected at the Z peak ($E_{\rm cm} \approx 91.2$ GeV) during the years 1992–1995.

The analysis of the present paper relies on comparisons of data with QCD model calculations. Monte Carlo events were generated using tuned parameters as given in Sect. 3. These events were passed through a full simulation of the ALEPH detector and were subject to the same reconstruction and analysis programs as the data. The numbers of hadronic Z decays generated for each of the models are given in Table 6. If in the following the GAL model is mentioned, the version with $R_0 = 0.10$ is implied unless stated otherwise.

6 Analysis of energy-ordered jets

6.1 Three-jet event selection

The Durham (or $k_{\rm T}$) cluster algorithm [32–34] is applied to the energy flow objects in order to determine the number of jets. The distance measure between any two particles is defined as

$$y_{ik} = 2\min(E_i^2, E_k^2)(1-\cos\theta_{ik})/E_{\rm vis}^2 = (2k_{\rm T}/E_{\rm vis})^2 \,.$$

A value of 0.02 has been chosen for the resolution parameter $y_{\rm cut}$ as a compromise between well separated jets and sufficient statistics. This value corresponds to $k_{\rm T,cut} = 6.5$ GeV for the case $E_{\rm vis} = E_{\rm cm}$. This analysis deals with events which have exactly three jets. Their fraction is 23% in data before any further cuts. Three-jet events in which more than 95% of any jet energy is carried by photons are assumed to be hard bremsstrahlung off quarks and are rejected (0.7% of the three-jet events). To improve the particle acceptance, the event is only kept if the angle θ_j of each jet with respect to the beam direction satisfies $|\cos\theta_j| < 0.90$.

Table 7. Some properties of energy-ordered jets in data

jet number	$\langle E_{\rm jet}\rangle$, GeV	spread, GeV	$\langle n_{\rm ch}\rangle$	$P_{\rm g}$
1	40.8	2.7	8.81	0.059
2	32.7	4.5	8.28	0.248
3	17.7	5.1	7.02	0.693

The jet energy resolution is improved by the following procedure. The jets are first ordered according to their observed energies, $E_1 > E_2 > E_3$. As the measured jet vectors in general do not exactly form a plane, an average plane is constructed by taking the vector $(\mathbf{p}_1 \times \mathbf{p}_3) + (\mathbf{p}_3 \times \mathbf{p}_2)$ as the normal to this plane. Jets 1 and 2 are projected into this plane. The jet energies are recomputed from the interjet angles assuming energy-momentum conservation for massless jets. The jets are then ordered again, but this time according to the computed jet energies such that $E_1 > E_2 > E_3$. As further kinematic cuts the smallest of the interjet angles is required to be greater than 40 degrees and the smallest of the scaled jet energies, $x_j = 2E_j/E_{\rm cm}$, to be greater than 0.1. These cuts only become important for resolution parameter values smaller than 0.02 used for systematic checks. All these criteria result in 539 000 three-jet events ($= N_{\rm 3j}$). Some of the jet properties are listed in Table 7.

The information on the shower development of JETSET Monte Carlo events is used to estimate the probability, $P_{\rm g}$, of a jet to be the gluon jet. The primary quarks from $Z \to q\bar{q}$ (after termination of the parton shower) are assigned to the reconstructed jets by means of the smallest angle. The jet which has no quark assigned to it is then called the gluon jet. The least energetic jet (jet 3) has an average computed energy of 17.7 GeV. It represents a gluon jet in about 69% of the cases. The highest energy jet (jet 1) is dominantly a quark jet with flavour composition given by the electroweak Z couplings. The selected sample comprises a wide range of kinematic configurations.

6.2 Jet charge distributions

The jet charge is defined here as the sum of the charges q_i (in units of the elementary charge) of the particles which are assigned to jet j by the cluster algorithm:

$$Q_j = \sum_{i=1}^{n} q_i = n_+ - n_- \qquad (2)$$

with n being the number of charged particles in the jet under consideration and $n_+(n_-)$ the number of particles with charge $+1$ (-1). This definition does not explicitly depend on the particle momenta. It has previously been used by the OPAL collaboration [35] in a study of quark and gluon jet charges.

The Q_j distribution is influenced by many factors. The charge of the underlying hard parton is expected to be reflected in the charges of the produced hadrons. Therefore the charge of a gluon jet should be zero on average. This is also true for quark-initiated jets because quarks are not distinguished from antiquarks in this analysis, which enter with equal frequency. An important property is the width of the distribution which depends on the mean particle multiplicity, on the jet environment and on the jet finder used. In addition the width is limited by local charge compensation in jet fragmentation. Also, Bose–Einstein correlations have an influence on the width. Experimental effects in general tend to smear and to shift the distribution.

The measured Q_3 distribution of jet 3 is shown in Fig. 1 for the full data sample, together with the JETSET prediction. The data are rather well described by the simulation, in particular the fraction of neutral $(Q_3 = 0)$ jets. The data distribution is not symmetric around 0, but slightly shifted towards positive values, a feature which is also reproduced by the simulation and which can be explained by protons from nuclear interactions in the detector material. The same is true for jets 1 and 2. The colour reconnection model GAL predicts a higher rate of neutral jets in the gluon-enriched jet (jet 3) than is seen in the data.

6.3 Rapidity gaps

The particle distribution in jets is analysed in terms of rapidity

$$y = \ln\left(\frac{E + p_{\mathrm{L}}}{\sqrt{m^2 + p_{\mathrm{T}}^2}}\right) .$$

The longitudinal and transverse momentum components (p_{L} and p_{T}) are measured with respect to the jet axis, which is defined as the vector sum of all energy flow objects assigned to the jet. The pion mass is assumed for all charged particles except for those identified as electrons or muons, where m_{e} or m_{μ} is used. Neutral particles are assumed to be massless. They are included only if their energy exceeds 0.6 GeV because of the poor agreement between data and simulation at low energies.

Figure 2 shows the multiplicity distribution of charged plus neutral particles, $n_{\mathrm{c+n}}(\Delta y)$, for jet 3 within a central rapidity interval $0 \le y \le y_{\mathrm{u}}$ with the upper limit chosen as $y_{\mathrm{u}} = 1.5$. About 7% of the jets in data have zero particles in this interval, as seen in the leftmost bin in the figure. In this bin the background from quark jets is relatively high (60% according to JETSET), because of their lower average multiplicity with respect to gluon jets. Starting from $y_{\mathrm{u}} = 1.0$, the rate of these 'gap-jets' falls nearly exponentially with increasing interval size. The rate is seen to be sensitive to CR effects: JETSET predicts too few and GAL predicts too many of these jets. The rate of jets with a rapidity gap obviously depends on the shape of the

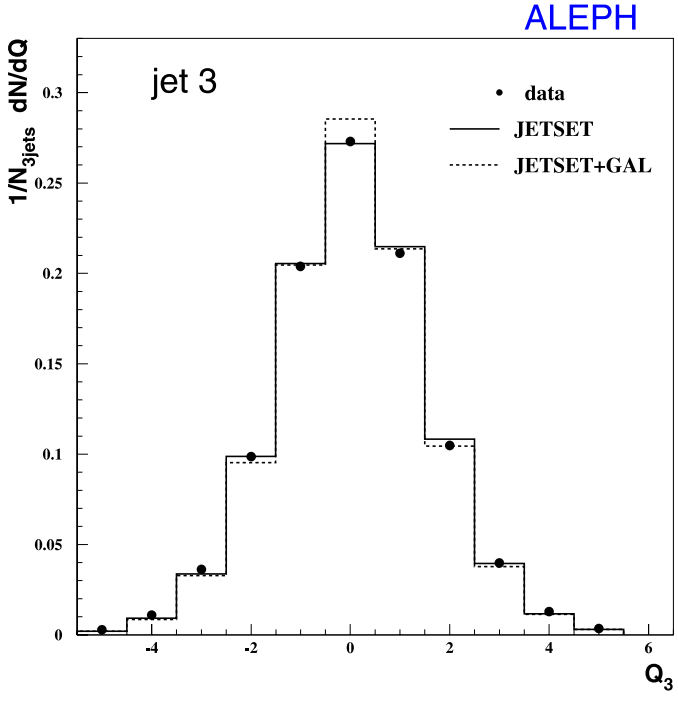

Fig. 1. The charge distribution of jet 3 (the lowest energy jet) compared to JETSET predictions without and with colour reconnection

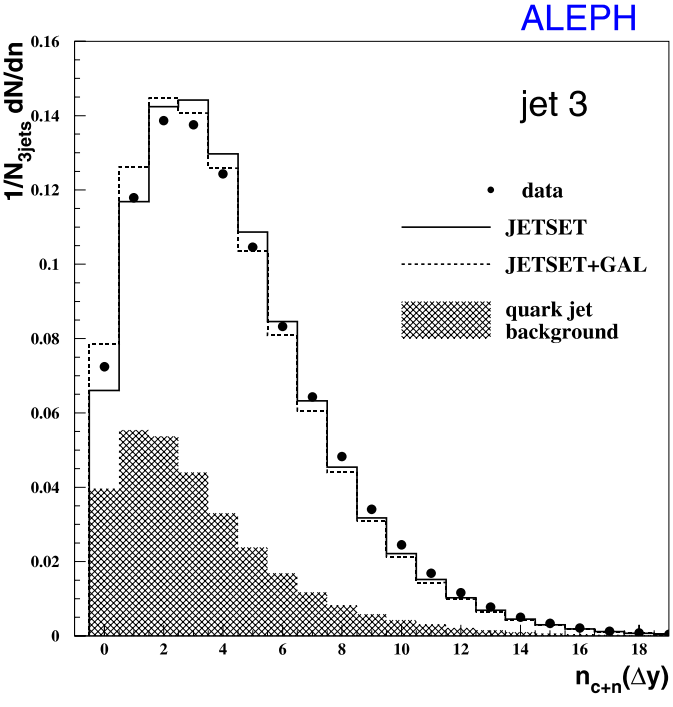

Fig. 2. The distribution of the number of charged plus neutral particles in the rapidity interval $0 \le y \le 1.5$ for jet 3, compared to JETSET without and with CR. The *hatched area* is the quark jet background as evaluated with JETSET

multiplicity distribution. The width of the distribution is slightly underestimated by the QCD models.

A second definition of a rapidity gap, based on the maximum rapidity distance, $\Delta y_{\max}$, between adjacent particles in a jet has been proposed in [8]. Since the system beyond the gap selected in this way is found to consist dominantly of one particle only and is found to be less sensitive to CR effects, it is not investigated further.

6.4 Charge distributions of jets with a rapidity gap

The charge distribution of jets which exhibit a central rapidity gap as defined above is shown in Fig. 3 for jet 3. The jet charge is computed from charged particles with rapidities $y > y_{\mathrm{u}}$. The fraction of particles moving backwards ($y < 0$) is negligibly small (of order 10^{-4}). The distribution is normalized to the total number of three-jet events, $N_{3\mathrm{j}}$, which means that the rate of gap-jets also enters into the comparison of data with Monte Carlo models. The distribution in Fig. 3 is narrower than the corresponding one for the full sample (Fig. 1) due to the smaller average particle multiplicity. The rate of neutral jets with a rapidity gap (Fig. 3) shows an even higher sensitivity to CR than the rate of gap-jets alone. None of the models agrees well with the data : while the GAL model predicts too many neutral jets, standard JETSET predicts too few of them.

The relative model–data differences of the rate $r(0)$ of neutral jets

$$\delta = \frac{r(0)_{\mathrm{MC}} - r(0)_{\mathrm{data}}}{r(0)_{\mathrm{data}}}\,,$$
$$\text{where} \quad r(0) = \frac{N(Q_j = 0, \Delta y\,\mathrm{gap})}{N_{3\mathrm{j}}} \qquad (3)$$

are shown in Fig. 4 for jet 3 as a function of the rapidity gap size. Note that the points are not statistically independent : each point represents a sub-sample of the previous point(s). Both the colour-reconnected and the standard versions of JETSET and ARIADNE are seen to diverge from the data with increasing gap size. For the case $y_{\mathrm{u}} = 1.5$, the GAL model deviates from the data by 17σ (statistical). The CR effect in the AR1 model is slightly weaker than that in the GAL model. Colour reconnection as implemented in these two models and assuming default values for the strength parameters, is therefore disfavoured by the data. The GAL model with a smaller value for the strength parameter, $R_0 = 0.04$, still gives somewhat too high predictions. On the other hand, the rates predicted by standard JETSET and ARIADNE (without CR) are systematically low if there is a rapidity gap. The quantity $r(0)$ has little or no sensitivity to the HERWIG-CR model, as can be seen from Fig. 5.

The δ values for the quark-enriched jet (jet 1) are shown in Fig. 6 for comparison. As expected, this jet shows very little sensitivity to CR for all models. The data are quite well described by JETSET. The ARIADNE model shows some deviation in the case of a gap. HERWIG is unable to describe the data. This is related to the observation that HERWIG's particle rapidity distributions are systematically lower over a wide range of rapidity and that the Q_j distributions are narrower than the corresponding data distributions.

The effect of Bose–Einstein correlations, as simulated with the tuned BE_{32} model, is to slightly broaden the charge distributions, leading to a downward shift of the δ

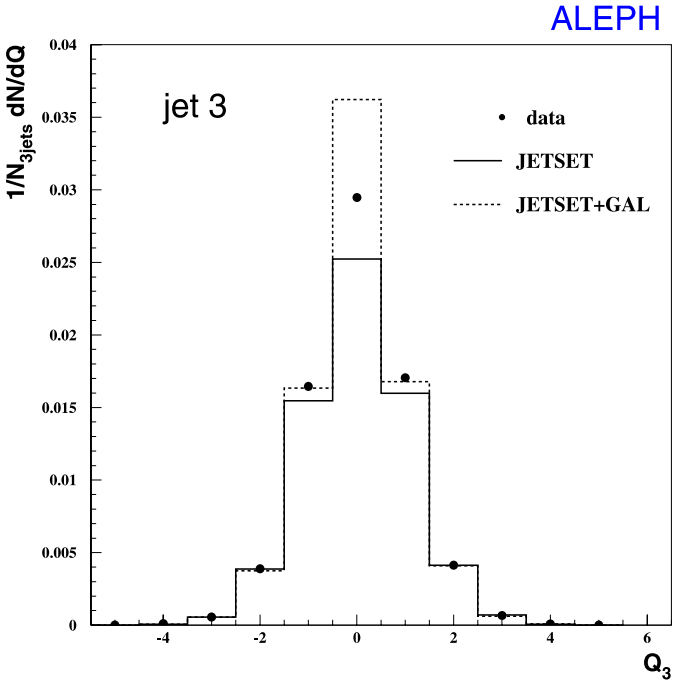

Fig. 3. The charge distribution of jet 3 for a rapidity gap in $0 \leq y \leq 1.5$

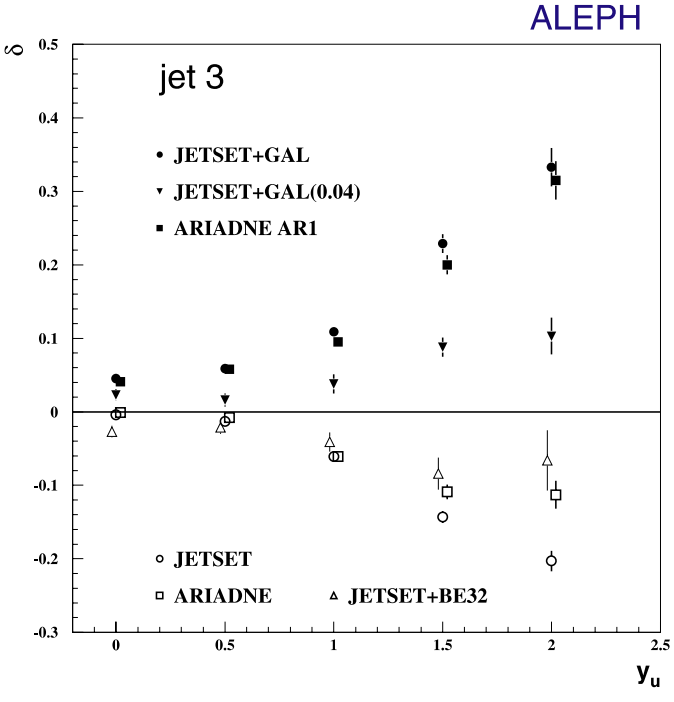

Fig. 4. The relative model–data differences δ in the rate $r(0)$ of neutral jets for jet 3 as a function of the upper limit of the rapidity gap. The points at $y_u = 0$ correspond to the full sample. Statistical uncertainties of the data and the Monte Carlo calculations are shown as error bars

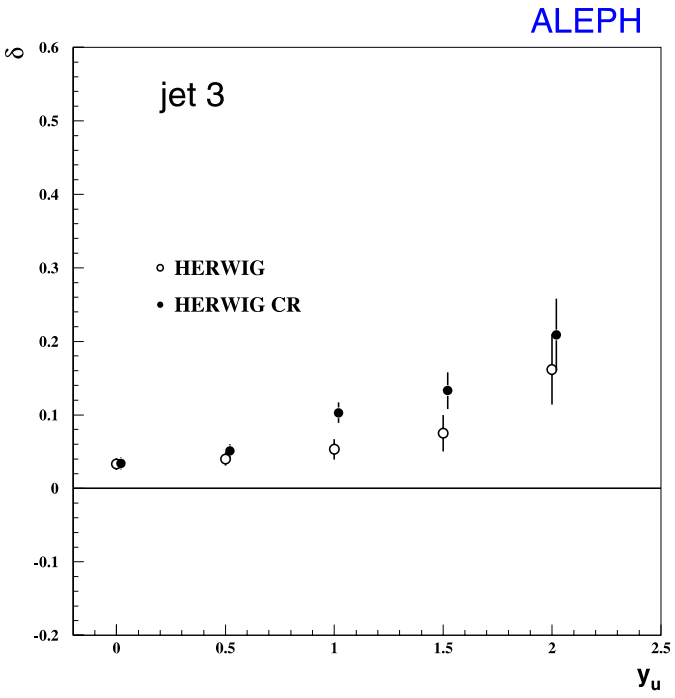

Fig. 5. The relative HERWIG–data differences δ in the rate $r(0)$ of neutral jets for jet 3 as a function of the upper limit of the rapidity gap

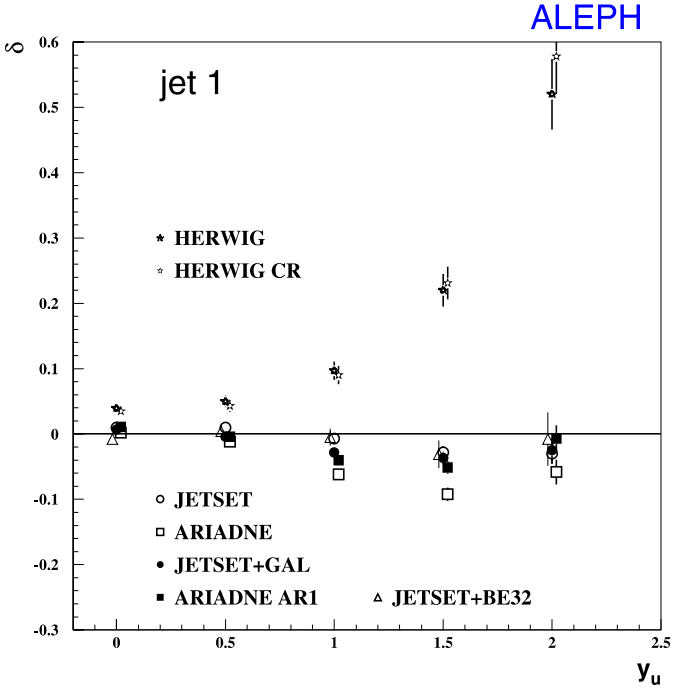

Fig. 6. The relative model–data differences δ in the rate $r(0)$ of neutral jets for jet 1 as a function of the upper limit of the rapidity gap. The points at $y_u = 0$ correspond to the full sample. Statistical uncertainties of the data and the Monte Carlo calculations are shown as error bars

values by about -0.02 for the full samples of jets 1 and 3. For events with a gap in jet 3 (Fig. 4) the shift in δ goes into the other direction.

The results are less dependent on model-data discrepancies in the multiplicity distributions if the Q_j distributions of jets with a rapidity gap are normalized to unit area for both data and Monte Carlo models. The quantity studied is the fraction of neutral jets

$$f(0) = \frac{N(Q_j = 0, \Delta y\,\text{gap})}{N(\Delta y\,\text{gap})}\,, \qquad (4)$$

where $N(\Delta y\,\text{gap})$ is the number of jets with a rapidity gap. The model-data differences are similar to those discussed above but statistically less significant. The predictions of the non-CR models JETSET and ARIADNE for the third jet are low also in this case, with a relative deviation from the data by about -6% for a rapidity gap in $0 \le y \le 1.5$, confirming the results of a similar analysis by DELPHI [11].

6.5 Corrected rate of neutral jets

The results presented so far indicate that none of the QCD models provides a satisfactory description of the data for jet 3 with a rapidity gap. If the data are to be described by a colour reconnection model, the question then arises which value of the CR parameter is required by the data. For this study, the parameter R_0 of the GAL model is considered, (1). In order to save computing time, the data are first corrected for the effects of the detector, of the reconstruction chain and the analysis cuts by means of a correction factor (C) derived from the JETSET simulation :

$$r(0)^{\text{corr}}_{\text{data}} = r(0)_{\text{data}} \cdot \frac{r(0)_{\text{MC,gen}}}{r(0)_{\text{MC,sim}}} = r(0)_{\text{data}} \cdot C\,, \qquad (5)$$

and similarly for $f(0)$. The calculation including full simulation of the detector is denoted as 'MC,sim'. The calculation at the particle level of the event generator ('MC,gen') is done separately according to the following prescription. Hadronic Z events are generated without initial- and final-state photon radiation. The Durham cluster algorithm is applied to all charged and neutral stable particles to select three-jet events. The jets are ordered according to their actual energies. Rapidities are calculated using the actual particle masses. To define a rapidity gap, neutral particles with energies smaller than 0.6 GeV are omitted.

The results for the lowest energy jet (jet 3) and requiring a gap in the rapidity range 0–1.5 are given in Table 8. The quoted systematic error arises from model dependence and is estimated by taking the largest difference of the results when correcting with JETSET, GAL(0.04) or ARIADNE. These numbers can then be compared to those obtained from generator level calculations of the JETSET+GAL model for different values of R_0. The complication here is that the CR effect is not a one-parameter problem : the fraction of reconnected events depends strongly on the parton shower cut-off, Q_0, but only very weakly on the fragmentation parameter b. To ensure agreement of the average particle multiplicity with the data, at each R_0 value the parameters Λ, σ and b are re-tuned to global quantities, while keeping Q_0 fixed at 1.5 GeV.

Table 8. Corrected data values for the rates of neutral jets in jet 3 with a rapidity gap from 0 to 1.5. The first error is statistical, the second systematic

	corrected data
$r(0)$	$0.0234 \pm 0.0004 \pm 0.0015$
$f(0)$	$0.437 \pm 0.006 \pm 0.010$

The comparison yields an optimal value for the colour reconnection parameter R_0 of about 0.02 if the quantity $r(0)$ is used, and about 0.01 if $f(0)$ is used.

7 b-tag analysis

A much higher gluon jet purity can be achieved by identifying both the quark and the antiquark jets in events of the type $Z \to b\bar{b}g$, by utilizing the long lifetime of B-hadrons [36]. Based on the three-dimensional impact parameter and its significance measured for each charged particle track the probability $P_{\rm jet}$ is computed that all charged tracks of a jet arise from the primary interaction vertex. The method of gluon-tagging is taken from [25, 26]. Three-jet events are selected in which two of the jets exhibit significant lifetime ($P_{\rm jet} < 0.01$), whereas the remaining jet does not ($P_{\rm jet} > 0.01$). This latter jet then represents the tagged gluon jet. No energy ordering is applied here.

The event selection and the computation of the jet energies are the same as already described in Sect. 6.1 except that all three jets are required to fall in the geometrical acceptance of the VDET ($|\cos\theta_j| < 0.766$) and that the scaled gluon jet energies, $x_{\rm g}$, are restricted to values smaller than 0.85.

The fraction of three-jet events surviving the lifetime tag condition alone is 7.6% in data, to be compared to 7.4% in the JETSET simulation. About 24 600 tagged three-jet events are selected from data. According to JETSET Monte Carlo calculations 95% of the events actually arise from primary b-quark pairs, 4.2% from c-quark pairs and the rest from light quark pairs. The tagged gluon jet energies are distributed with mean value 19.8 GeV and a spread of 7.8 GeV. The tagged gluon jet is estimated to be the 'true' gluon jet in 97.2% of the cases on average. Since the gluon purity is found to drop rapidly at high energies, the scaled jet energies are restricted to values $x_{\rm g} \leq 0.85$ as mentioned above. A sub-sample of 18 700 tagged gluon jets are lowest energy jets. This sub-sample is therefore included in the jet-3 sample of the energy-ordered analysis presented in Sect. 6.

In order to test colour reconnection models the same analysis is performed on the tagged gluon jet as on the least energetic jet in Sect. 6. Due to the higher gluon purity the results are expected to be less dependent on the quark jet background in the sample. Figure 7 shows the charge distribution of the tagged gluon jets. The rate of neutral ($Q_{\rm g} = 0$) jets is well described by JETSET. The CR model predicts a clear excess with respect to the data. Figure 8 shows the multiplicity distribution of charged plus neutral particles within the central rapidity interval $0 \leq y \leq 1.5$.

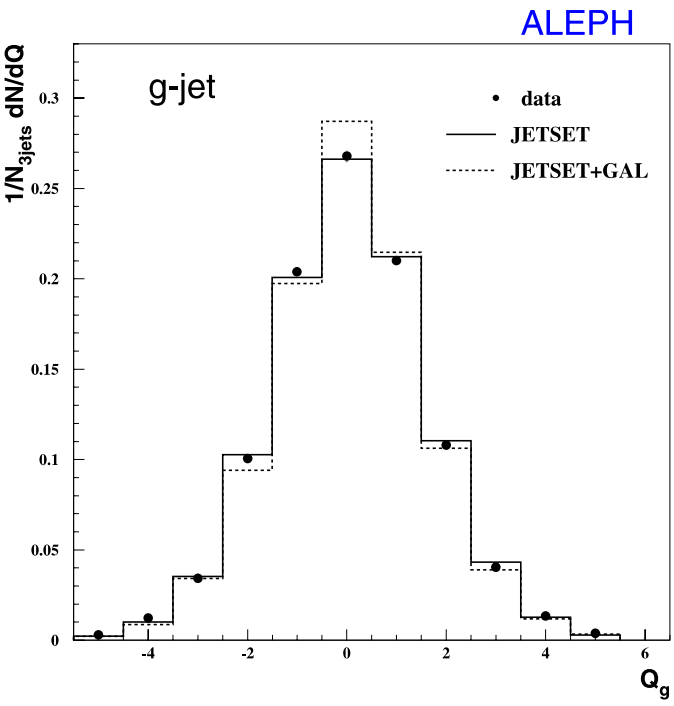

Fig. 7. The charge distribution of anti-b tagged gluon jets compared to JETSET predictions without and with colour reconnection

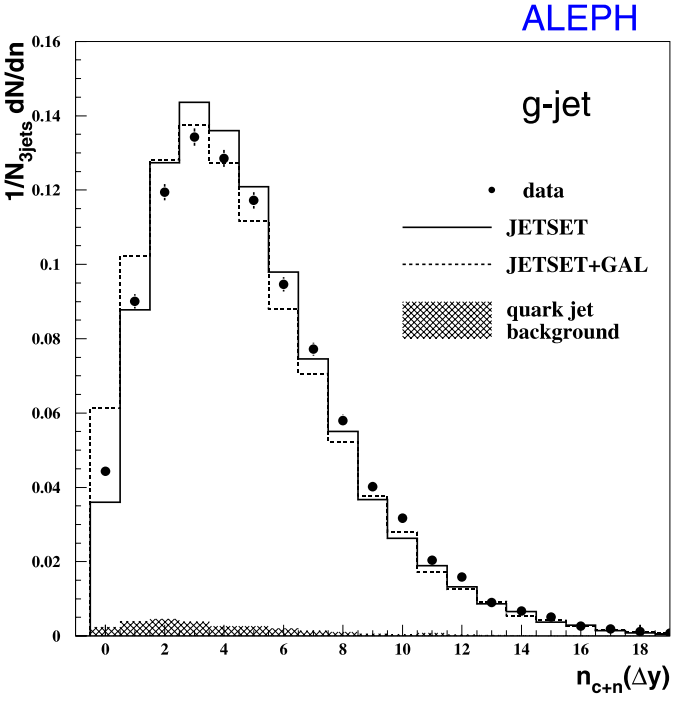

Fig. 8. The distribution of the number of charged plus neutral particles in the rapidity interval $0 \leq y \leq 1.5$ for anti-b tagged gluon jets, compared to JETSET without and with CR. The hatched area is the quark jet background as evaluated with JETSET

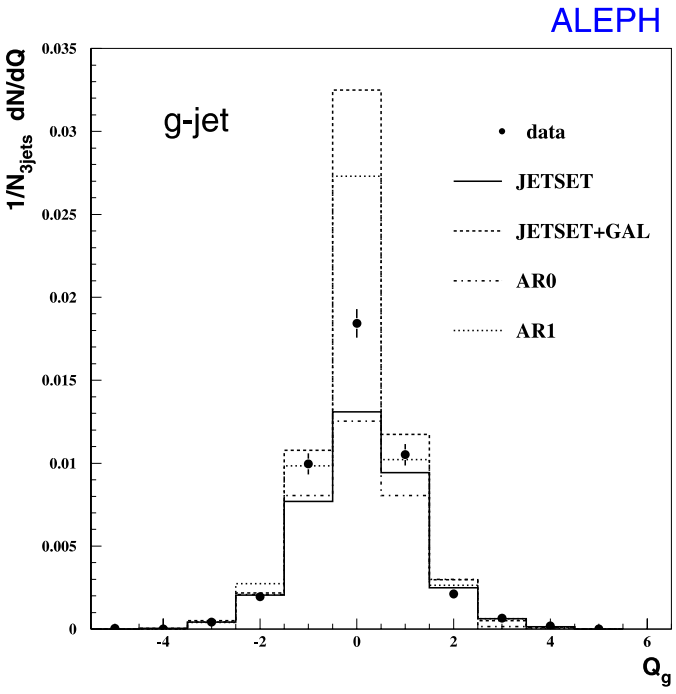

Fig. 9. The charge distribution of anti-b tagged gluon jets with a rapidity gap in $0 \leq y \leq 1.5$

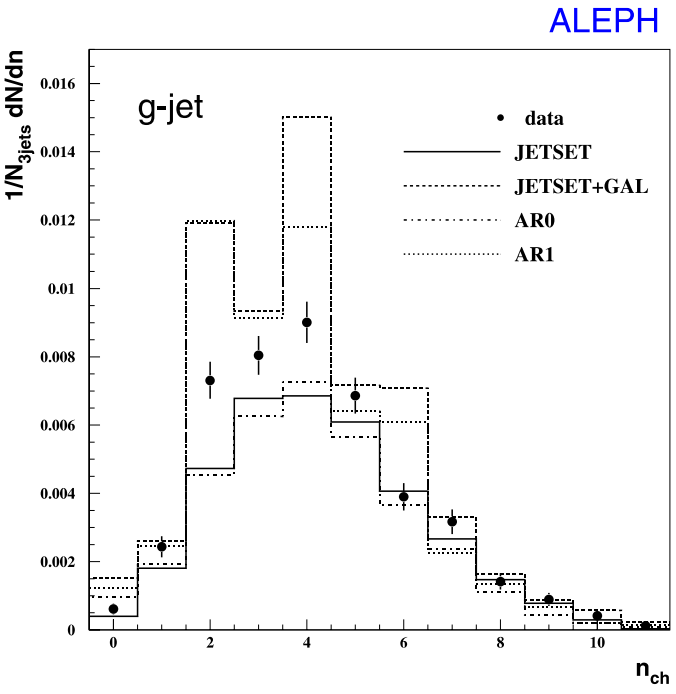

Fig. 11. The charged multiplicity distribution of anti-b tagged gluon jets with a rapidity gap in $0 \leq y \leq 1.5$

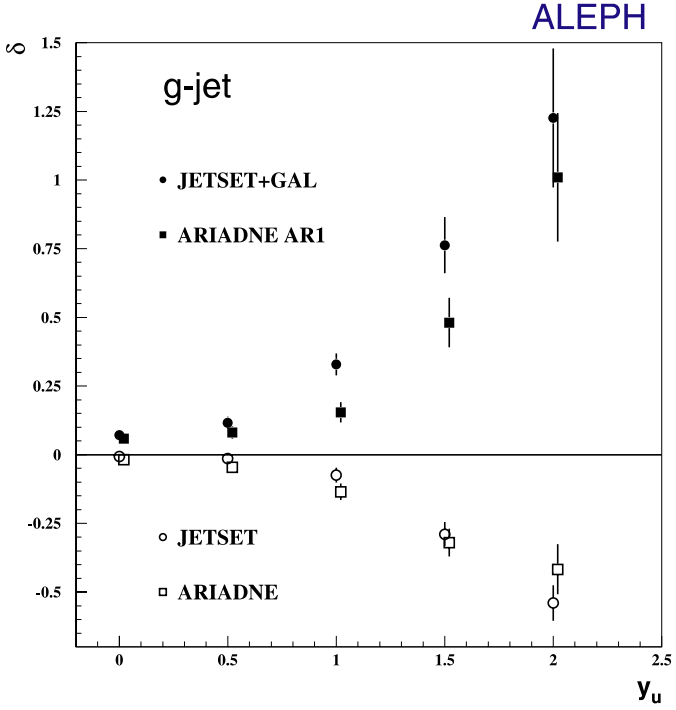

Fig. 10. The relative model–data differences δ in the rate $r(0)$ of neutral jets as a function of the upper limit of the rapidity gap for the anti-b tagged gluon jet. The points at $y_u = 0$ correspond to the full sample. Statistical uncertainties of the data and the Monte Carlo calculations are shown as error bars

The rate of jets having zero particles in this interval (rapidity gap) shows sensitivity to CR. The gluon purity for those jets is still high (93.5%).

The charge distribution of the jets exhibiting a rapidity gap is shown in Fig. 9. This distribution is normalized to the number of tagged three-jet events and contains 1090 jets in data. Clearly, the CR models GAL and AR1 predict too many neutral gluon jets. The relative model–data differences δ (Fig. 10) are numerically larger than those from the energy-ordered analysis and reach values around 1. The results of the b-tag analysis confirm those of the energy-ordered analysis although with less statistical significance. At $y_{\rm u} = 1.5$ the GAL model deviates from the data by about 7σ (statistical).

The distribution of the charged track multiplicity in gluon jets with a rapidity gap is shown in Fig. 11. The data do not exhibit clear evidence for spikes at the even values $n_{\rm ch} = 2$, 4 and 6 as predicted by the CR models GAL and AR1.

8 Systematic checks

The energy-ordered analysis has been repeated by varying the definition of the jets and the definition of the rapidity gap in the following ways :

- The Durham jet resolution parameter, $y_{\rm cut}$, has been varied in the range from 0.01 to 0.03.
- A different jet finder, the JADE algorithm, has been used with resolution parameter $y_{\rm cut} = 0.08$, which leads to a similar three-jet event rate.
- A re-assignment of particles to jets was performed on the basis of the smallest angle with respect to the jet axes. Afterwards the jet four-momenta are recomputed. This mainly affects particles at large angles

Table 9. Experimental cuts varied for systematics studies

cut	standard value	changed value
$\|d_0\|$, (cm)	2.0	0.5
$\|z_0\|$, (cm)	10.0	5.0
N_{TPC}	4	6
$\|\cos\theta_j\|$	0.90	0.80

to the jet axes which are of importance for defining a rapidity gap.
– The rapidity gap has been defined with charged tracks only.
– The shifted rapidity regions (0.5–1.5) and (1.0–2.0) were also used to define the gap.

In all five cases the qualitative features of the results remain the same, although the numerical values of the measured quantities may change.

Possible inadequacies of the detector simulation have been studied by varying, in data and simulation, some of the cuts on the charged tracks and the cut on the polar angle of the jet axes according to Table 9. This has been done only for the normalized jet charge distributions. In all cases, the model–data differences only change within their statistical errors.

The model–data comparison of the rate of jets with a rapidity gap relies on the calibration of the average particle multiplicity at the detector level. In all hadronic events, the average charged particle multiplicity, $\langle n_{\mathrm{ch}}\rangle$, of all generators, including HERWIG, agrees with the data to an accuracy below 1% which, of course, is a result of the model parameter tuning. For JETSET and ARIADNE this also holds for three-jet events, and in addition for each of the three jets individually. In contrast, HERWIG exhibits a 1.5%–2.5% deficit in each of the three jets of three-jet events, thus giving less reliable predictions.

9 Conclusions

Three-jet final states from e^+e^- annihilation into hadrons are used to test QCD models of colour reconnection (CR). From a sample of approximately 3.4 million hadronic Z decays, collected by the ALEPH detector at LEP, three-jet events are selected by the k_{T} cluster algorithm with a fixed cut-off, $y_{\mathrm{cut}} = 0.02$. The distributions of particle multiplicity in jets in fixed rapidity intervals and the distributions of the jet charge are investigated. The main analysis is based on jet energy ordering. According to JETSET, the least energetic jet (jet 3) represents a gluon jet in about 69% of the cases.

Gluon jets with a large gap in rapidity and with zero electric charge of the system beyond the gap constitute a particularly sensitive test. The rate, $r(0)$, of these jets is measured as a function of the rapidity gap size and is compared to predictions of globally tuned QCD generators. The rate $r(0)$ is predicted too high by the string-based CR models JETSET+GAL and ARIADNE AR1 when using default values for the CR strength parameters. Thus these two models are disfavoured by the data as already observed in [8]. On the other hand, the rate is too low for the standard, non-CR versions of these generators, in agreement with a similar analysis in [11]. The R_0 parameter of the GAL model is constrained by the data to the range 0.01–0.02. The quantity $r(0)$ turns out to be insensitive to CR as implemented in the HERWIG-CR model.

In a separate analysis of the same data, two b-quark jets are positively identified using lifetime tagging, thus achieving a very high gluon jet purity of about 97% for the remaining jet. The results confirm those of the energy-ordered analysis though with less statistical significance.

Assuming that the physics of colour rearrangements is similar in hadronic Z decays and in WW decays, this result would imply that the CR models as implemented in JETSET+GAL and ARIADNE overestimate the systematic shift of the measured W boson mass.

Acknowledgements. We wish to thank our colleagues from the CERN accelerator divisions for the successful operation of LEP. We thank L. Lönnblad, J. Rathsman, T. Sjöstrand and B.R. Webber for discussions on the theoretical aspects. We are indebted to the engineers and technicians in all our institutions for their contribution to the excellent performance of ALEPH. Those of us from non-member states wish to thank CERN for its hospitality.

References

1. G. Gustafson, U. Pettersson, P.M. Zerwas, Phys. Lett. B **209**, 90 (1988)
2. The LEP Collaborations and the LEP electroweak working group, A combination of preliminary electroweak measurements and constraints on the standard model, Eprint hep-ex/0511027, CERN-PH-EP/2005-051
3. L3 Collaboration, Phys. Lett. B **561**, 202 (2003)
4. OPAL Collaboration, Eur. Phys. J. C **45**, 291 (2006)
5. OPAL Collaboration, Eur. Phys. J. C **45**, 307 (2006)
6. ALEPH Collaboration, Eur. Phys. J. C **47**, 309 (2006)
7. C. Friberg, G. Gustafson, J. Häkkinen, Nucl. Phys. B **490**, 289 (1997)
8. OPAL Collaboration, Eur. Phys. J. C **35**, 293 (2004)
9. OPAL Collaboration, Eur. Phys. J. C **11**, 217 (1999)
10. L3 Collaboration, Phys. Lett. B **581**, 19 (2004)
11. M. Siebel, Study of the charge of leading hadrons in gluon and quark fragmentation, In: Proc. XXXXth Rencontres de Moriond (QCD and Hadronic interactions at high energy), La Thuile, 12–19 March 2005, hep-ex/0505080, paper in preparation
12. P. Minkowski, W. Ochs, Phys. Lett. B **485**, 139 (2000)
13. T. Sjöstrand, V. Khoze, Phys. Rev. Lett. **72**, 28 (1994)
14. T. Sjöstrand, V. Khoze, Z. Phys. C **62**, 281 (1994)
15. T. Sjöstrand et al., Comput. Phys. Commun. **135**, 238 (2001)
16. T. Sjöstrand, private communication
17. L. Lönnblad, Comput. Phys. Commun. **71**, 15 (1992)
18. L. Lönnblad, Z. Phys. C **70**, 107 (1996)
19. J. Rathsman, Phys. Lett. B **452**, 364 (1999)

20. T. Sjöstrand, Comput. Phys. Commun. **82**, 74 (1994)
21. G. Corcella et al., JHEP **0101**, 010 (2001) [hep-ph/0011363]
22. ALEPH Collaboration, Physics Reports **294**, 1 (1998)
23. G. Rudolph, Colour reconnection in W pairs and Monte Carlo tuning at LEP, In: Proc. XXXVth Rencontres de Moriond (QCD and high energy hadronic interactions), Les Arcs, 18–25 March 2000
24. ALEPH Collaboration, Phys. Lett. B **606**, 265 (2005)
25. ALEPH Collaboration, Eur. Phys. J. C **17**, 1 (2000)
26. ALEPH Collaboration, Phys. Lett. B **346**, 389 (1995)
27. ALEPH Collaboration, Phys. Lett. B **384**, 353 (1996)
28. DELPHI Collaboration, Eur. Phys. J. C **13**, 573 (2000)
29. OPAL Collaboration, Eur. Phys. J. C **37**, 25 (2004)
30. ALEPH Collaboration, Nucl. Instr. Meth. A **294**, 121 (1990)
31. ALEPH Collaboration, Nucl. Instr. Meth. A **360**, 481 (1995)
32. S. Catani et al., Phys. Lett. B **269**, 432 (1991)
33. N. Brown, W.J. Stirling, Z. Phys. C **53**, 629 (1992)
34. S. Bethke, Z. Kunszt, D.E. Soper, W.J. Stirling, Nucl. Phys. B **370**, 310 (1992)
35. OPAL Collaboration, Phys. Lett. B **302**, 523 (1993)
36. ALEPH Collaboration, Phys. Lett. B **313**, 535 (1993)